

CONFERENCES AND SYMPOSIA

PACS number: 01.10.Fv

Scientific session of the Physical Sciences Division of the Russian Academy of Sciences "Methods of wave-based physics in neuroscience problems and applications" (31 October 2007)

A scientific session of the Physical Sciences Division of the Russian Academy of Sciences (RAS) was held under the title "Methods of wave-based physics in neuroscience problems and applications" on October 31, 2007 in the conference hall of the P N Lebedev Physical Institute, RAS. The following reports were presented at the session:

(1) **Nekorkin V I** (Institute of Applied Physics, RAS, Nizhny Novgorod) "Nonlinear oscillations and waves in neurodynamics";

(2) **Bezruchko B P** (Department of Nano- and Biomedical Technologies, Saratov State University, Saratov), **Ponomarenko V I, Prokhorov M D, Smirnov D A** (Saratov Branch of the Institute of Radioengineering and Electronics, RAS, Saratov), **Tass P A** (Juelich Research Center, Institute of Neuroscience and Biophysics 3-Medicine, Juelich, Germany) "Modeling nonlinear oscillatory systems and diagnostics of coupling between them using chaotic time series analysis: applications in neurophysiology".

An abridge version of the reports is given below.

PACS numbers: **05.45.–a**, 05.45.Xt, **87.10.+e**
DOI: 10.1070/PU2008v051n03ABEH006493
DOI: 10.3367/UFNr.0178.200803g.0313

Nonlinear oscillations and waves in neurodynamics

V I Nekorkin

1. Introduction

1.1 Nonlinear dynamic approach

The past decade has witnessed an increasing integration of the methods of nonlinear dynamics into neuroscience — a marriage of ideas that has produced a number of interesting results on the dynamics of neuron systems and enabled many forms of neuron activities to be adequately interpreted in terms of dynamical systems theory. Concepts such as regular and chaotic attractors, stability, the attraction region, and bifurcation have come to be firmly incorporated into the conceptual framework for the entire field of research on various aspects of brain activity by the methods of nonlinear dynamics. The emergence of this field is quite easy to explain. First, significant advances in neuron activity detection techniques (including optical neuroimaging, positron emission tomography, magnetic resonance imaging and some others) have brought about a massive amount of experimental data on how neurons, alone or in a system, operate. These data formed the basis for launching a variety of modern studies on the nonlinear dynamics of neuron systems. Second, the theory of dynamical systems has also developed considerably. By now, among other things, nonlinear waves and localized states have been investigated for many types of spatially distributed systems and the bifurcation theory of multidimensional dynamical systems has by and large been constructed (in particular, the transition from deterministic to chaotic behavior has been studied rather thoroughly). And third, finally, the operation regime features and the very evolutionary nature of neuron systems stimulate neuroscience applications of nonlinear dynamics methods. Indeed, the characteristic features of neuron systems are as follows:

(a) dissipative dynamics;

(b) external sources arising from complex biochemical processes and acting to compensate losses;

(c) neurons being active elements capable of generating a variety of electric oscillations, from simple single pulses to chaotic ones.

On the other hand, features (a) to (c) are characteristic of so-called self-oscillatory (or autooscillatory) systems — a major class of systems with which nonlinear physics is concerned. The conceptual framework of the theory of self-oscillatory systems was created by A A Andronov, who indeed introduced the very notion of self-sustained oscillations and who showed that periodic oscillations are adequately imaged by Poincaré limit cycles whose bifurcations describe and explain nonlinear mechanisms by which various forms of periodic oscillations and beats are created and disappear in many physical systems. Although the modern theory of self-oscillations shifted its focus to more complicated, in particular, chaotic oscillations, its underlying dynamical principles remain the same as stated by A A Andronov [1 – 3]. These are:

(1) the separation and study, first and foremost, of structurally stable (robust) systems and phenomena, whose behavior remains fundamentally unchanged by small variations in the system parameters (i.e., the study of general situations);

Uspekhi Fizicheskikh Nauk **178** (3) 313 – 329 (2008)
DOI: 10.3367/UFNr.0178.200803f.0313
Translated by E G Strel'chenko; edited by A Radzig

(2) the analysis of the way the phase space of the system (or the space of its states) is partitioned into trajectories. This is primarily the study of the attractors (equilibrium states, limit cycles, invariant tori, chaotic limit sets), as well as of homoclinic and heteroclinic orbits and invariant separatrix manifolds with the aim of describing all the possible types of behavior of the system;

(3) the study of how wave-oscillatory processes evolve with control parameters and the identification of the bifurcations that determine the fundamental rearrangement of these processes.

In our view, neuron systems constitute a reasonable and appealing application area for the principles listed above. The biological implications of self-oscillations were already noted by A A Andronov who, in his famous work "Poincaré limit cycles and the theory of self-sustained oscillations", wrote the following when citing examples of self-oscillatory systems: "...in mechanics [this is] the Froude pendulum; in physics, the electron-tube oscillator; in chemistry, periodic reactions, and similar problems arise in biology". However, the development of the nonlinear dynamical approach for application to neuron systems had its difficulties, due to the bizarre and complex nature of such systems. The following are only a few of the complexities faced [5 – 8]: the large number of variables and parameters needed to describe even a small ensemble of neurons or indeed a single neuron; the large number of complex and mostly nonlocal bonds between neurons; unlike many physical systems, neuron systems are not amenable to modeling from first principles, i.e., based on certain well-known and commonly accepted fundamental equations, such as Maxwell equations, and, in many cases, a poor understanding of the architecture of neuron systems and how they interact between themselves. Nevertheless, despite these and many other difficulties which we leave unnamed, the nonlinear dynamical approach already has been successfully used and is continuing to be effectively developed at present (as reviewed, for example, in Refs [8 – 14]).

To conclude, the main task of the nonlinear dynamical approach is to use neurophysiological data to develop adequate dynamic images of the key phenomena occurring in neuron systems and then using these images to develop — and study the dynamics of — some basic models. With this approach, it should be possible to describe, explain, and predict spatio – temporal processes that can occur in individual neuron ensembles, as well as to establish the system-level dynamic mechanisms that govern the operation of neuron systems and are crucial for developing the next generation of computing and information systems based on the principles of neurodynamics.

1.2 Basic properties of neurons

A neuron, also known as a nerve cell, typically consists (see, for example, Refs [5 – 8]) of a cell body, branching from which are many relatively short thin tubular fibers (dendrites) and one much longer fiber, the axon. Separating the neuron from its environment is a biological membrane. In the state of rest, the potential difference between the intracell medium and the outer surface of the membrane (henceforth simply membrane potential) has a negative value of order -60 to -80 mV and is called the rest potential. The function of dendrites is to receive signals from other neurons, whereas the axon serves to transmit to other neurons the signals generated by the given neuron. The axon ends with numerous terminal fibers which can contact the dendrites, axon, or body of another neuron. The so-called synapses by which the contact is implemented are a kind of device consisting of two (pre- and postsynaptic) membranes of the contacting neurons and the so-called synaptic slit — the gap between the membranes. Synapses come in two forms, electrical and chemical. In an electrical synapse, the pre- and postsynaptic membranes are in direct contact, thus enabling direct ion exchange and thereby making the membrane potentials of the contacting neurons equal.

In chemical synapses, biochemical processes occur in the synaptic slit and the contacting membranes. If the neuron potential exceeds a certain critical value (the excitation threshold) — whether due to the action of an outside stimulus or intracell processes — then the neuron produces what is called an action potential, an electric pulse with an amplitude of about $+50$ mV and a time scale of several milliseconds, and makes a transition into the so-called refractory state which is insusceptible to outside influences. The axon and the terminal fibers are the channels through which the action potential goes to the synaptic terminal, leading to a very special chemical substance, the neuromediator, being released into the synaptic slit. Having arrived at the postsynaptic membrane, the neuromediator changes its permeability to various ion species, which, in turn, causes the postsynaptic membrane potential to change. Depending on whether this moves the postsynaptic potential closer to or farther away from the excitation threshold, one distinguishes between excitatory and inhibitory (suppressing) synapses. The response of a neuron to the action of input signals is an integrated process: when the exciting and suppressing inputs combined reach the threshold value, the neuron produces a response which is transmitted to other neurons via the axon and synapses. Chemical synapses transmit excitation with a certain time delay due to processes occurring in the synaptic gap.

1.3 Typical forms of neuron activity

The electrical activity of neurons comes in a variety of forms, from a single action potential known as a spike (see Fig. 1a), to burst oscillations, i.e., 'volleys' of spikes occurring on the depolarization wave (Fig. 1b), to periodic oscillations of various kinds (Fig. 1c), to chaotic sequences of bursts (Fig. 1d), and to some others. Collective neuron activities are also widely diverse. The possible activities of neuron systems include the propagation of nonlinear waves (Fig. 1e); the formation of 'activity clusters', i.e., neuron groups that produce action potentials simultaneously while neighboring neurons are relatively at rest (Fig. 1f), and the formation and propagation of localized structures, to mention but a few.

1.4 Dynamic neuron models

There exist a quite large number of dynamic neuron models differing in both their target phenomena and in how completely their underlying neurophysiological data are used. Several distinctive groups of models can be identified.

(1) Models based on equations describing ion transport through the nerve cell membrane. First, these include, of course, the classical Hodgkin – Huxley model [20] and its extensions incorporating additional ion currents in the system, all the models being narrowly specific to the type of neuron. Second, there are simplified phenomenological models with a single variable describing the action of several ion flows of a similar typical time scale. A model with two variables, one for slow and the other for fast ion flows, is a

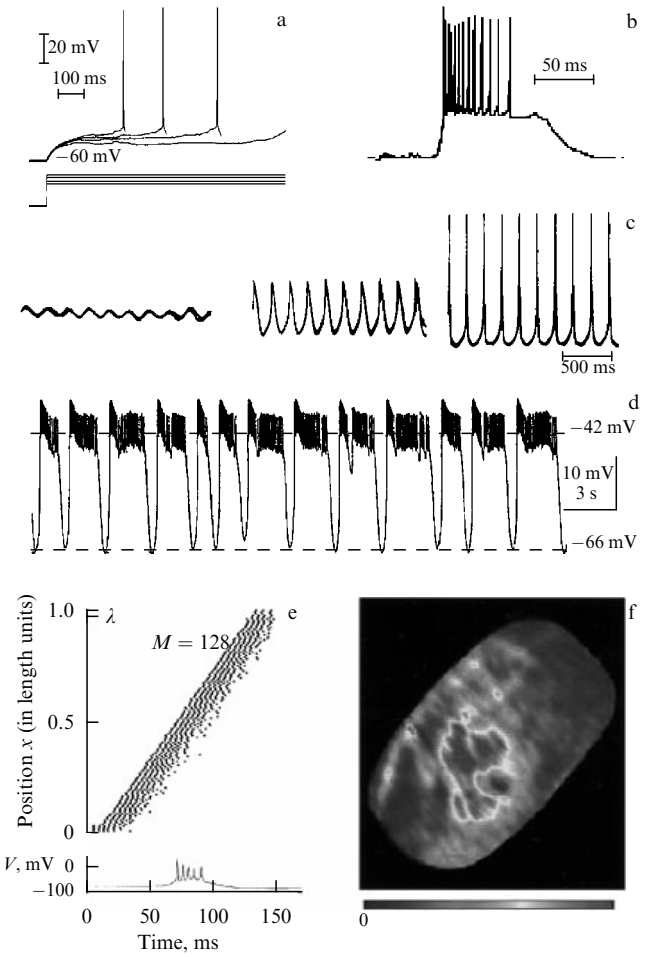

Figure 1. (a) Spike generation by pyramidal neurons of the visual cortex of a rat under *in vitro* conditions [15]. (b) Burst oscillations of a reticular neuron [15]. (c) Three activity forms of inferior olive neurons: subthreshold oscillations, and low- and high-threshold pulses. Data were obtained from the inferior olive neurons of a guinea pig, sliced *in vitro* [16]. (d) Chaotic burst oscillations of a lateral pyloric neuron [17]. (e) 'Discharge' waves in the brain cortex [18]. (f) Clusters in an ensemble of inferior olive neurons [19]. The color gradation is used to indicate membrane potential distribution in the ensemble.

frequent example typified by the Hindmarsh–Rose system [21] for describing burst oscillations. Moreover, in some models, like those of FitzHugh–Nagumo [22, 23], Morris–Lecar [24], etc., a single 'recovery' variable is used to describe the action of all the ion flows involved.

(2) Integrate-and-fire models (see, for example, Ref. [25]) primarily focused on the integral properties of neurons. A model system accumulates input signals until, under their combined action, the variable modeling membrane potential reaches the threshold value, at which moment this variable is given a certain fixed value which is treated as a spike. After that the value of the membrane potential is returned to the initial state of rest.

(3) Mean field models operating with variables averaged over the neuron ensemble. The Wilson–Cowan model [26], for example, has two variables — one for the number of excitatory neurons, and the other for the number of inhibitory neurons at a given point in the medium.

(4) Phase models comprising first-order equations whose variables are angular and treated as oscillation phases (phase rotator [27, 28], 'theta neuron' [29], etc.). These highly simplified models are commonly used to study synchronization regimes in large nonlocally linked neuron ensembles.

(5) Models in the form of nonlinear point maps have also been utilized [30–33]. Such models are time discrete but, unlike cell automata, their state is continuous. These models have a simpler structure than those described by a system of differential equations. It is established that while point mappings are capable of modeling many regimes of neuron activity, their most appealing application is in studying chaotic neuron oscillations.

While the above list is of course by no means exhaustive, we believe it gives a sufficient idea of the basic objectives and concepts of the dynamic approach to the study of neuron activities.

Modeling neuron systems requires a dynamical description of synaptic bonds and of the general architecture of the system, in addition to modeling individual neurons. The simplest to model are electrical synapses (see, for example, Ref. [7]), whose operation relies on the existence of so-called gap junctions between neurons in contact. Due to this junction, in a certain narrow region the cell membrane becomes common to the two neurons, so that the current through the synaptic bond is determined by the junction's resistance and the potential difference between the neurons, and is modelled by the ordinary Ohm law. Chemical synapses are usually described (see, for example, Refs [14, 34]) by a special kind of differential equations for their parameters, the equations involving nonlinear threshold functions. The architecture of dynamic models reflects the organization of actual neuron systems and varies widely, from small ensembles of neurons to multilayered neuron networks and populations consisting of a large number of elements coupled by numerous nonlocal bonds.

2. The oscillatory and wave dynamics of FitzHugh–Nagumo neuron ensembles with nonlinear recovery

A key problem in the dynamics of neuron systems is the study of the forms of activity and mechanisms of propagation of activity arising locally in a certain part of the system. Following Refs [35, 36], let us consider this problem for an ensemble of FitzHugh–Nagumo (FHN) neurons localized on the sites of a one-dimensional spatial lattice (chain) and connected by electrical synapses. The collective behavior of such a neuron ensemble is described by a system of equations

$$\begin{aligned} &\dot{u}_j = f(u_j) - v_j + d(u_{j-1} - 2u_j + u_{j+1})\,, \\ &\dot{v}_j = \varepsilon\big[g(u_j) - v_j - I\big]\,, \\ &j = 1, 2, \ldots, N\,, \qquad u_0(t) \equiv u_1(t)\,, \qquad u_{N+1}(t) \equiv u_N(t)\,, \end{aligned} \tag{1}$$

where j is the number of the element (neuron), N is the number of elements in the ensemble, the variable u_j describes qualitatively the membrane potential dynamics of the jth neuron, and v_j is the combined action of all the ion flows which pass through the membrane of this neuron and which are responsible for the recovery of the state of rest of the membrane. The parameter d models the action of the electrical synapse and quantifies the interneuron interaction. The parameter I controls the membrane's depolarization level, and ε ($\varepsilon > 0$) is the rate of change of the ion currents. The cubic function $f(u)$ and the (monotonically increasing) function $g(u)$ are respectively specified as [37] $f(u) = u - u^3/3$

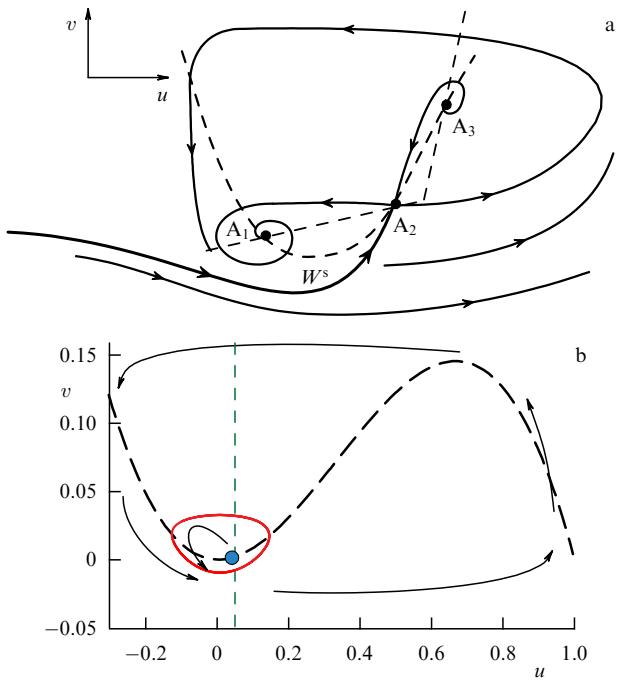

Figure 2. (a) Phase portrait of an element (neuron) in ensemble (1). (b) Phase plane of system (4).

and $g(u) = \alpha u$ for $u < 0$, and $g(u) = \beta u$ for $u \geqslant 0$, where α and β ($\alpha, \beta > 0$) describe the nonlinear dependence of the ion flows on the cell membrane potential (nonlinear recovery).

We choose (see Refs [37, 38]) the parameters of an element of system (1) such that the element possesses the property of excitability (Fig. 2a). In this case, the phase plane (u, v) of an individual element exhibits a stable equilibrium state A_1 corresponding to the neuron's state of rest; a saddle A_2 whose stable separatrix W^s determines the neuron's excitation threshold, and an unstable equilibrium state A_3. Applying (and subsequently removing) an above-threshold external stimulus produces in the phase plane (u, v) a trajectory which returns to A_1 by enclosing the equilibrium state A_3 (Fig. 2a). To this trajectory there corresponds a single excitation pulse (or spike) of the neuron, whose shape is controlled by the parameter ε.

2.1 Chaotic excitation of an ensemble

Because the active elements of system (1) are located at the sites of a one-dimensional spatial lattice, the index j can be treated as the spatial coordinate, and the dynamics of system (1) are spatio – temporal. Let us consider the propagation of activity in system (1) in the form of wave patterns whose typical spatial scales are much larger than those of the system itself — that is, a sufficiently large number of lattice elements is present along the characteristic length of a pattern. In this approximation, the dynamics of the wave patterns are described by the system of equations

$$\begin{aligned} \dot{u} &= y\,, \\ \dot{y} &= \frac{c^2}{d}\left[y - f(u) + v\right], \\ \dot{v} &= g(u) - v - I\,, \end{aligned} \tag{2}$$

where the over-dot denotes differentiation with respect to the 'running coordinate' $\xi = t - j/c$.

Let us show that the complex wave patterns of ensemble (1) are associated with the existence in system (2) of heteroclinic contours formed by the separatrix manifolds of the equilibrium states of system (2) [39]. For the parameter values for which the elements of ensemble (1) exhibit the dynamics shown in Fig. 2a, system (2) has three equilibrium states of the saddle-focus type. Two of these states, O_1 and O_3, have an unstable one-dimensional manifold and a stable two-dimensional manifold, whereas the third one, O_2, has a stable one-dimensional manifold and an unstable two-dimensional manifold (Fig. 3a, d).

The study of system (2) showed that the trajectories of the invariant manifolds of these equilibrium states can form homo- and heteroclinic orbits, when the parameters belong to certain bifurcation sets. Furthermore, it was found that in the parameter space of system (2) there exists the bifurcation set C of codimension 2, to which there corresponds in the phase space the heteroclinic contour depicted in Fig. 3a. In the parameter plane (ε, c), this set is represented by point C (Fig. 3b), which is asymptotically approached by two spiral-shaped bifurcation curves Γ and H centered on it. To the points of the curve Γ there correspond homoclinic trajectories formed by the one-dimensional separatrix of the point O_1, which returns to O_1 by 'enclosing' the point O_3. As the separatrix moves along Γ to point C, it performs an ever increasing number of oscillations in the vicinity of point O_2. To the points of set H there correspond heteroclinic trajectories formed by the separatrix of the saddle-focus O_1, a separatrix which asymptotically approaches point O_3. Here, too, the separatrix oscillates in the vicinity of point O_3 as the parameters of H are varied toward the spiral's center. Because homoclinic trajectories are doubly asymptotic with respect to one and the same equilibrium state, nonlinear waves in the form of traveling pulses correspond to them in ensemble (1) (see Ref. [39]). The wave fronts of the ensemble correspond to the heteroclinic trajectories 'linking' various equilibrium states [39]. The shapes of the wave profiles involved depend on the oscillatory properties of the appropriate trajectories. Moving along curves Γ and H to point C, the wave motion profiles become more complicated, and for parameter values close to the center of the spirals system (1) has a denumerable set of various wave motions at the same time. Because the branches of spirals Γ and H go close to each other, the waves differ only slightly in velocity. The existence of a large number of various wave motions in this region of parameters leads to the formation of complex wave structures in system (1).

It was established that only the lowest-velocity pulses (the lowest branch of curve Γ in Fig. 3b) can be stable. All the other traveling waves, including pulses with complex shapes and all the wave fronts, turned out to be unstable. This might well be expected because the spatially uniform states O_2 and O_3 are unstable in the parameter range of interest. The spatio – temporal diagram in Fig. 3c displays a typical activity propagation scenario for ensemble (1). The parameter ε was chosen to have a value close to the first turning point of curve Γ (Fig. 3b), and the initial activity of the ensemble to have the form of the wave front. Because of the instability this front decomposes into a series of excitation pulses which, as time goes on, also lose stability and decompose into a pair of wave fronts or a pair of pulses, followed, as the instability develops, by decomposition into another pair of pulses, etc. (Fig. 3b). These wave instabilities lead to spatio – temporal chaos, which develops due to the

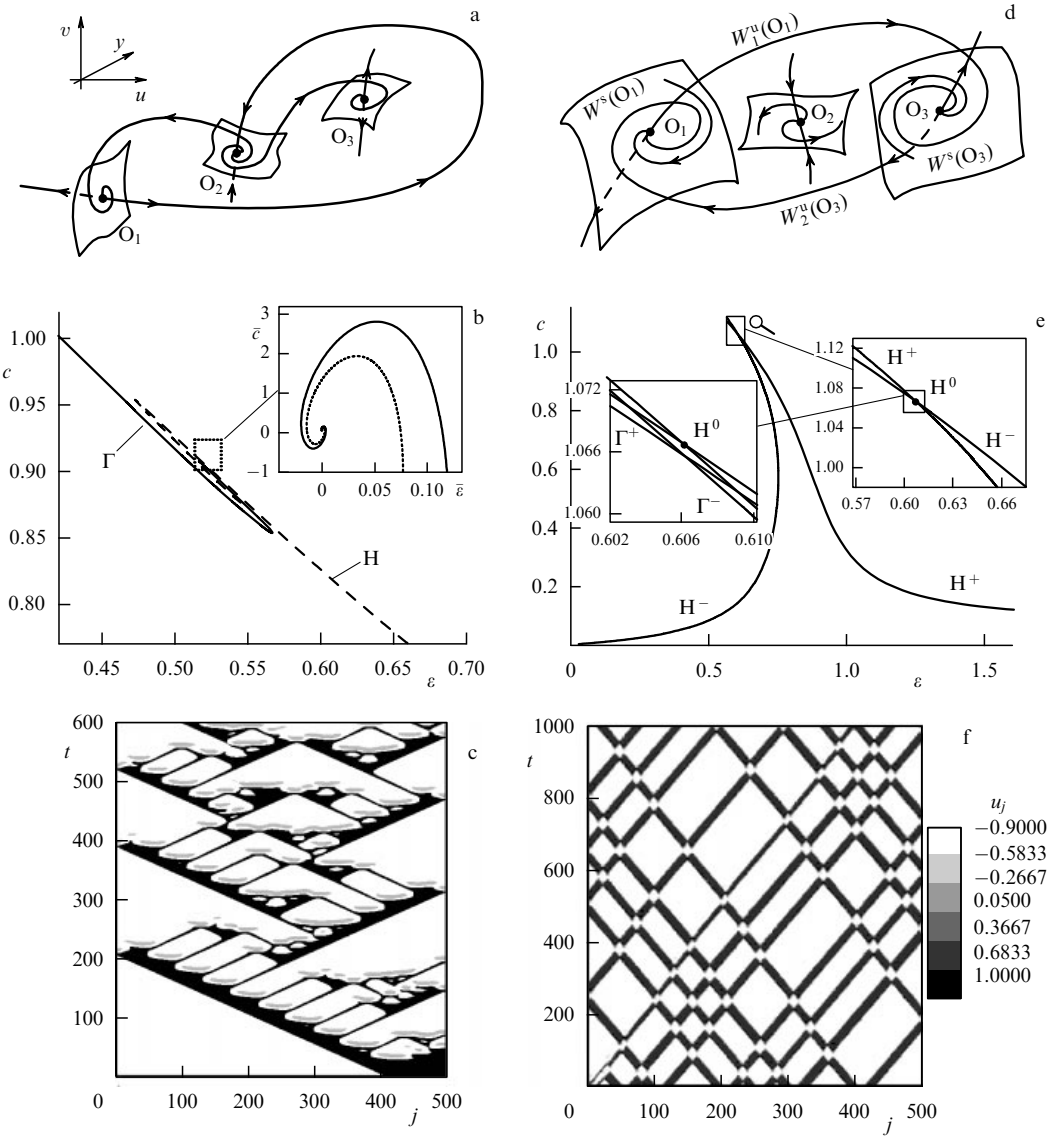

Figure 3. (a) Heteroclinic contour corresponding to the bifurcation set C. (b) Propagation velocities of pulses (curve Γ) and wave fronts (curve H) for ensemble (1). Parameters are as follows: $\alpha = 0.5$, $\beta = 2$, and $I = 0.2$. (c) Spatio – temporal chaos in ensemble (1). Parameters are as follows: $\alpha = 0.5$, $\beta = 2$, $I = 0.2$, $d = 1$, and $\varepsilon = 0.57$. (d) Heteroclinic contour corresponding to the bifurcation set $H^0(\varepsilon^0 = 0.60593, c^0 = 1.0664)$. Parameters are as follows: $\alpha = 0.9$, $\beta = 0.8$, $I = 0.24$, and $d = 1$. (e) Propagation velocity curves for wave fronts (curves H^+, H^-) and pulses (curves Γ^+, Γ^-). Parameters are the same as in figure d. (f) Spatio – temporal activity diagram of ensemble (1). Parameters are as follows: $\alpha = 0.9$, $\beta = 0.9$, $I = 0.024$, $d = 1$, and $\varepsilon = 0.585$.

existence of a countable number of unstable traveling waves. In other words, the system passes from the vicinity of one unstable wave to that of another, forming a spatio – temporal structure in doing so.

2.2 Self-replicated wave patterns

System (2) can exhibit other heteroclinic contours [40, 41], to which there also correspond complex wave patterns in ensemble (1). Figure 3d depicts a heteroclinic contour formed by manifolds of only two (not three, as in Section 2.1) equilibrium states (O_1 and O_3). In the plane (ε, c), this contour exists at the point H^0 (Fig. 3e), the interlocking point for the bifurcation curves H^+ and H^- that correspond to heteroclinic trajectories formed by the separatrices $W_1^u(O_1)$ and $W_2^u(O_3)$ (Fig. 3d) of the equilibrium states O_1 and O_3. Moreover, in the vicinity of point H^0 bifurcation curves Γ^+ and Γ^- (Fig. 3e) exist, to which there correspond homoclinic trajectories formed by the respective separatrices $W_1^u(O_1)$ and $W_2^u(O_3)$ of the saddle-foci O_1 and O_3. Note that both at the moment of existence of these homoclinic trajectories and at the moment when they are destroyed there exists in the phase space of system (2) a nontrivial hyperbolic set which includes an infinite number of periodic trajectories and some others. Hence, for parameter values from the vicinity of H^0 the system (2) exhibits extremely complex dynamics for traveling waves, suggesting that the spatio – temporal behavior of ensemble (1) should also be nontrivial in this case. Numerical simulations have shown that this is indeed the case. For values of ε close to $\varepsilon = \varepsilon^0$ (Fig. 3e), wave pulses and wave fronts 'pass' through one another and are reflected from the boundary similar to the way classical solitons are. As a result, complex wave patterns having the property of 'self-reproducibility' form in ensemble (2). Figure 3f illustrates the formation and propagation of such wave activity patterns emerging from several regions of the ensemble local excitation.

3. Activity clusters and self-phase reset

The information characteristic that is of crucial importance in the study of neuron systems is the oscillation phase. It is the oscillation phase which determines the instants of time when action pulses, or spikes, are produced, which are believed to be the basis of the 'neuron code' and to perform various functions of transmitting and transforming information. For example, inferior olive neurons, which form the basis for the olive-cerebellar system, display quasiperiodic membrane potential oscillations below the excitation threshold (the left panel of Fig. 1c), with a fixed amplitude of 5 to 10 mV and a fixed frequency of 8 to 12 Hz [16]. Varying the level of depolarization of an inferior olive neuron produces excitation pulses at the peaks of subthreshold oscillations. There are two different excitation thresholds involved. Reaching the first (lowest) threshold at each peak of subthreshold oscillations causes the neuron to generate a broad pulse with a relatively small (~ 20 mV) amplitude (the central panel of Fig. 1c). The appearance of such pulses is essentially determined by the flows of Ca^{2+} ions. Reaching the second threshold, the neuron generates narrow high-power ($\sim 60-120$ mV) pulses (the right panel of Fig. 1c), whose formation is predominantly controlled by the flows of Na^{+} ions. Because the excitation pulses for an inferior olive neuron occur at the peaks of the subthreshold signal, the instants of time they appear are uniquely determined by the oscillation phase.

Thus, the collective activity structures of inferior olive neurons can be classified as phase clusters [42]. Current physiological thinking is that these phase clusters determine motor patterns, which in turn set muscular contraction patterns [43, 44]. For example, the in-phase oscillations of neurons determine the simultaneous appearance of action pulses, or spikes, and hence the synchronous contraction of certain muscle groups. The oscillation phase of an inferior olive neuron — and, hence, the configuration of phase clusters — changes when a sensory or command stimulus acts on the system.

Figure 4a illustrates a series of responses of an inferior olive neuron to an action of the external stimulus. Each time the stimulus acts it changes the phase of subthreshold oscillations, but in such a way that the oscillations always return to a same-phase state, with the value of the phase being independent of the instant when the stimulus arrives (initial phase) and being determined only by the amplitude and duration of the stimulus. By analogy with self-sustained oscillations, this effect was termed self-phase reset [45, 46].

3.1 Dynamic model and inferior olive neuron regimes

To explain the dynamic activity mechanisms of inferior olive neurons, the following phenomenological model was introduced [46]:

$$\varepsilon_{\mathrm{Na}}\,\frac{\mathrm{d}u}{\mathrm{d}t} = f(u) - v\,, \qquad (3)$$

$$\frac{\mathrm{d}v}{\mathrm{d}t} = v - d(z - I_{\mathrm{Ca}} - I_{\mathrm{Na}})\,,$$

$$\frac{\mathrm{d}z}{\mathrm{d}(kt)} = f(z) - w\,, \qquad (4)$$

$$\frac{\mathrm{d}w}{\mathrm{d}(kt)} = \varepsilon_{\mathrm{Ca}}\bigl(z - I_{\mathrm{Ca}} - I_{\mathrm{st}}(t)\bigr)\,.$$

The model consists of two interacting blocks, whose respective dynamics are determined by the variables (z, w) and (u, w). The first block, system (4), describes relatively slow processes in the neuron membrane, ones that are determined by the calcium component of the ion currents involved. This system forms quasisinusoidal subthreshold membrane potential oscillations. The second block, system (3), describes the generation of action potentials (or spikes), where sodium and potassium components of ion flows play a dominant role. The nonlinear function f has the form $f(x) = x(x - a_{\mathrm{Ca,\,Na}})(1 - x)$, $0 < a_{\mathrm{Ca,\,Na}} < 1$. The parameters $I_{\mathrm{Ca,\,Na}}$ characterize the depolarization levels and control the excitation thresholds of the appropriate components of the model. The parameter k determines the relative time scales of the blocks. The interaction between the blocks is controlled by the coupling parameter d, and the interblock coupling itself is unidirectional. The parameters of system (3), (4) are chosen such that system (4) generates quasistationary self-oscillations corresponding to the limit cycle (Fig. 2b) in the vicinity of the Andronov – Hopf bifurcation. System (3) abides in the excitable regime and on exceeding a certain threshold generates short-duration excitation pulses. The function $I_{\mathrm{st}}(t)$ serves to describe the action of external stimulation.

In the absence of a stimulus ($I_{\mathrm{st}} \equiv 0$), system (4), which sets the basic oscillatory rhythm of the model, influences system (3) via a periodic signal. Hence, the dynamics of (3) are not autonomous and can be described by a Poincaré point map generated by trajectories of the system (3). A numerical study of the Poincaré map revealed the existence of parameter values for which system (3) executes stable periodic motion in the three-dimensional nonautonomous phase space. Because $\varepsilon_{\mathrm{Na}} \ll 1$, the dynamics of system (3) turn to be relaxational: the variable v varies much more slowly with time than the variable u.

This behavior of the variables has the consequence that the three-dimensional phase space of system (3) is partitioned into regions of slow motion and those of fast motion. Depending on the value of the coupling constant, the periodic motion of system (3) is either fully localized in a slow-motion region or consists of parts of slow- and fast-motion regions. There exist two threshold values for the coefficient d, which determine the respective numbers of slow- and fast-motion regions contributing to the formation of the periodic trajectory of system (3). Below the first of the two thresholds, the periodic trajectory of system (3) is fully localized in a slow-motion region, and corresponding to it are nearly sinusoidal periodic oscillations that are in-phase oscillations of the first block. In this case, the oscillations of system (3) (see the left panel of Fig. 4b) model the subthreshold oscillations of the inferior olive neurons. Overcoming the first threshold results in the periodic trajectory of the system (3) having, in addition to a part from the slow-motion region, a part from the fast-motion one. To this periodic trajectory there will correspond oscillations which have short pulses at each peak of the subthreshold oscillations (see the central panel of Fig. 4b) and which can be treated as excitation pulses from the lower threshold (Ca^{2+}-pulses) of an inferior olive neuron. Above the second threshold, the periodic trajectory of system (3) has two slow-motion regions 'linked' by a fast-motion one, with the passage time through the second slow-motion region being much shorter than that through the first region forming the 'subthreshold pedestal'. In this case, to the

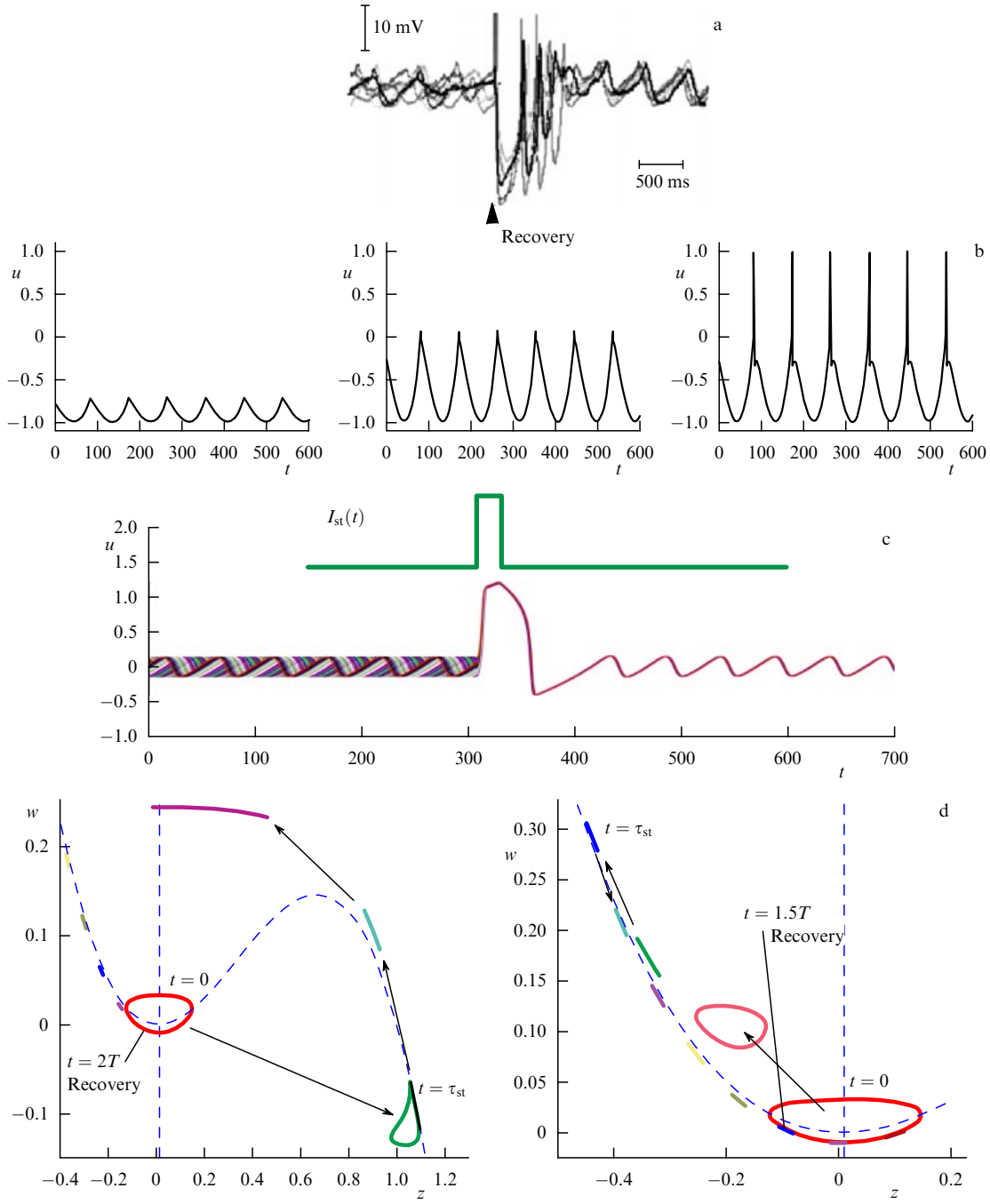

Figure 4. (a) Self-phase reset effect in inferior olive neurons. Data were obtained from rat brain stem slices [19]. (b) Oscillations of inferior olive neurons for model (3), (4). (c) Self-phase reset in system (4). Waveforms of the oscillations for various initial conditions (synchronization with a stimulus pulse). Parameters are as follows: $A_{st} = 1.15$, and $\tau_{st} = 0.4\,T$, where T is the subthreshold oscillation period. (d) Dynamic mechanism of self-phase reset in the phase plane (z, w). Stimulus-driven transformation of the closed limit-cycle curve. Sequence of snapshots of a hundred initial conditions uniformly distributed along the limit cycle prior to the stimulus action. Left: excitatory ($A_{st} = 1.15$, $\tau_{st} = 0.4\,T$) stimulus. Right: inhibitory ($A_{st} = -1$, $\tau_{st} = 0.4\,T$) stimulus.

periodic trajectory of system (3) there correspond oscillations at whose peaks there occur pulses with several times the amplitude of the pulses from the lower threshold (see the right panel of Fig. 4b). These oscillations quite adequately describe the two-threshold generation of (Na^+-pulse of) an inferior olive neuron.

To conclude, system (3), (4) enables one to model all basic activity regimes of inferior olive neurons, yielding a good qualitative agreement with available experimental data (compare Figs 4b and 1c).

3.2 Self-phase reset

In addition to the activity regimes of an inferior olive neuron, it turns out [45–47] that system (3), (4) allows the effect of self-phase reset to be modelled (Fig. 4a). Because the subthreshold oscillations and instants of time of the pulse generation are in phase with the oscillations of the first block, the self-phase reset effect is in fact related to the dynamics of system (4) experiencing an external stimulus.

Let stimulus $I_{st}(t)$ be a single pulse of amplitude A_{st} and duration τ. Note first that after the pulse ceases, system (4) has

the phase portrait shown in Fig. 2b, implying that the amplitude and frequency of the system's oscillations 'recover', assuming the values determined by the limit cycle of the system. However, the action of an external stimulus results in the phase of the recovered oscillations changing from its initial value φ_1 to φ_2.

Let the initial phase φ_1 be varied within the interval $[0, 2\pi]$. Referring to Fig. 4c, which shows the waveforms of the oscillations in system (4) for various initial phases, we see that stationary oscillations have virtually the same phase for any value of the initial phase. To characterize the distribution of the resettled phases, the unity-normalized standard deviation $\delta\varphi$ of the spread of these phases was plotted as a function of the stimulus pulse amplitude [45, 47]. For one hundred initial phases considered this function was found to be bell-shaped with the tails falling off rapidly on either side. For a sufficiently low-amplitude pulse, no phase reset occurs and the phase variable remains distributed in the interval $[0, 2\pi]$, with $\delta\varphi \approx 1$. As the amplitude $A_{\rm st}$ becomes larger than the threshold value, the resettled phases go through high localization around a certain average value $\varphi^*(A_{\rm st})$, with $\delta\varphi$ dropping off sharply and then decreasing monotonically to zero (for example, $\delta\varphi \approx 0.02$ for $A_{\rm st} = 3$). Notice that the phase reset occurs irrespective of whether the amplitude of the pulse is positive, $A_{\rm st} > 0$ (see Fig. 4c), or negative, $A_{\rm st} < 0$. In other words, phase reset occurs both in the case of an excitatory stimulus and in the case of an inhibitory action on the neuron. An exciting pulse provides a more 'precise' resetting, though.

Because $\varphi(A_{\rm st})$ can assume any value in the interval $[0, 2\pi]$, it is possible by appropriately choosing the amplitude of the pulsed action to preassign any value to the oscillation phase of system (3), (4), no matter what its prestimulation value was. Underlying the dynamic mechanism of self-phase resetting is the strong compression of the phase volume of the system (see Fig. 4d), due to the relaxation nature ($\varepsilon_{\rm Ca} \ll 1$) of system (4) — with the result that the system in fact 'forgets' its initial conditions.

3.3 Phase clusters of prescribed configuration

Here, we follow Refs [46, 47] and consider an ensemble of noninteracting inferior olive neurons, each of which is described by the system of equations (3), (4). Due to the self-phase reset effect it is possible to form phase clusters of any preassigned spatial configuration in this ensemble. By properly choosing the intensity of the stimulus, the phase of each element can be set equal to the desired value, independent of the current state.

Figure 5 illustrates how phase clusters are formed. The application of a stimulus causes the phases of the elements to group according to the 'cell' configuration stimulus. Notice that cluster formation does not require that the elements interact directly. Such interaction can be introduced to maintain the prescribed configuration during the time when the stimulus is absent. This is the way in which, for example, the olive-cerebellar system functions [16].

In the absence of a stimulus, inferior olive neurons interact via the gap junction, which makes them mutually synchronous. As a stimulus arrives, the inhibitory feedback loop acts to suppress the gap junction, and under the action of the sensor stimulus (Fig. 4a) the desired phase values of the elements are established. Formed in this way, the motor pattern of an arbitrarily complex spatial configuration provides the required synchronism of muscular contractions. The groups of muscles corresponding to a phase cluster contract simultaneously.

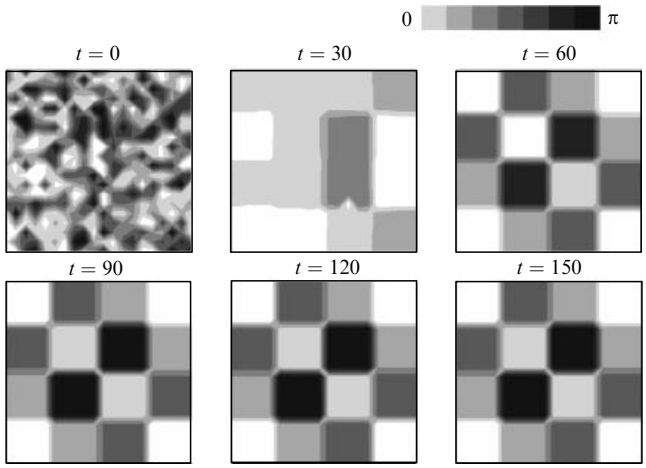

Figure 5. Phase cluster formation by means of self-phase reset in the ensemble of 20×20 noninteracting inferior olive neurons (3), (4). At the initial instant of time, a single stimulus pulse of duration $\tau_{\rm st} = 0.4\,T$ simultaneously acts on the random phase-distributed elements. A color gradation is used to indicate oscillation phase distribution in the ensemble.

Thus, the effect of self-phase reset is in fact a sensomotoric transformation in which the intensity of a sensor stimulus is converted to the motion-controlled pattern of muscular contractions.

4. Neurodynamics-based system of motor control and coordination of motions

As already noted in Section 3, inferior olive neurons are the key element of the olive-cerebellar system, the system which controls and coordinates motions and specifies the universal rhythm of muscular contractions. According to Refs [43, 48], any motion, rather than being continuous, is in a certain (kinematic) sense successive — that is, it has a characteristic time scale determined by the frequency of subthreshold oscillations, which is about 10 Hz. What the existence of this scale implies is that the nervous system with the aid of the olive-cerebellar system exercises its control over muscular contractions not more often than once in 100 ms, thus reducing the 'computation resources' required for motor control and imparting to the motion certain 'elasticity' in terms of precise tunability, adaptation to external conditions, etc. One of the key dynamic mechanisms involved in the olive-cerebellar system implementing the functions of control and operation is using the phase reset effect to form preconfigured phase clusters in an ensemble of inferior olive neurons. Based on this mechanism and using dynamic model described by equations (3), (4), a neurodynamic model for discretely controlling and coordinating the motion of autonomous robotic machines was proposed (Fig. 6a) [46, 49].

The control system of a walking robot (with six limbs, for example) has as its primary task to ensure that the machine moves stably along a rough surface. The idea of the control system proposed is to introduce a discrete control block to reflect the functions of inferior olive neurons. In this particular case, the single-neuron model (3), (4) was used to implement the block. The function of the control block is as follows. The block generates control pulses at a fixed frequency of 10 Hz, in the intervals between which the

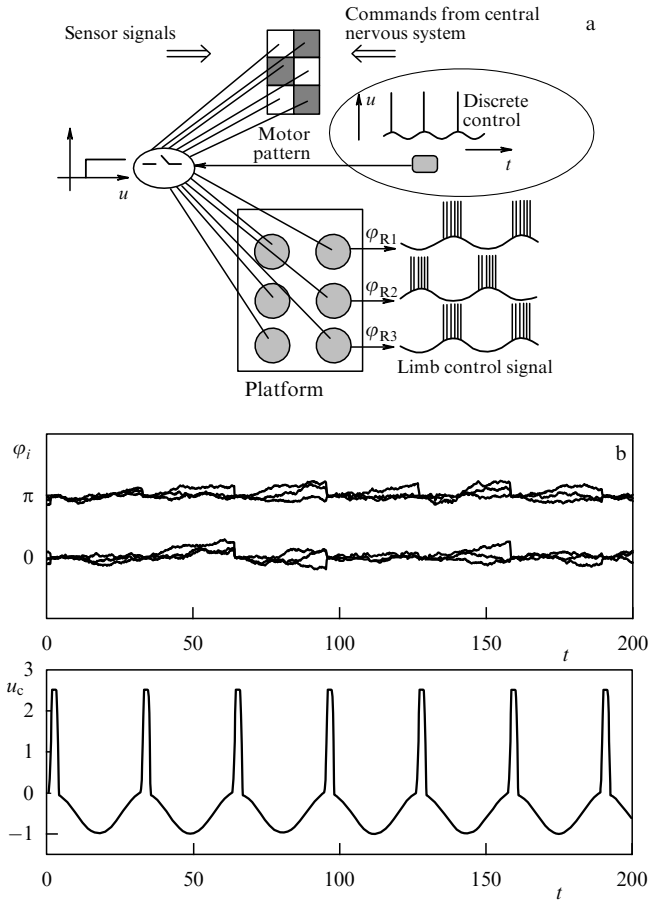

Figure 6. (a) Schematic of discrete motion control for a walking robot, using the self-phase reset effect. (b) Upper panel: limb phase control for a six-legged robot; phases are for two groups differing by π. Lower panel: control signal.

limbs of the robot adapt to the surface conditions unaided, due to various local self-tuning mechanisms which we leave out of consideration here. When pulses arrive, the limbs' positions are monitored and the phase relations ('motion pattern') securing walking stability are recovered. In particular, for a six-limbed robot to be stable, three of its limbs should be on the surface at any instant of time. Suppose that each of the limbs is controlled by a certain quasiperiodic signal whose phase uniquely determines the position of the robot's leg at each instant of time. Then the task of the control system reduces to mutually coordinating six phase variables. For this purpose, let us introduce the following dynamical system:

$$\dot{\varphi}_i = h\Phi(t, t_k, \Delta t)(\varphi_i^* - \varphi_i) - \xi_i\,, \qquad i = 1, 2, \ldots, 6\,, \qquad (5)$$

where φ_i is the phase of the given limb, and φ_i^* is the 'reference phase' which is specified in accordance with the motion pattern chosen. The function Φ modeling the operation of the discrete control block has the form

$$\Phi(t, t_k, \Delta t) = \begin{cases} 0\,, & t < t_k\,, \\ 1\,, & t_k < t < t_k + \Delta t\,, \end{cases} \qquad (6)$$

where t_k is the arrival time of the kth control pulse generated by system (3), (4) at the peaks of subthreshold oscillations with period T_c. The time period t during which the control system operates after each pulse is sufficiently short, $t \sim 0.1T_c$. The random uncorrelated quantities ξ_i are uniformly distributed over a certain interval $[-\xi_0, \xi_0]$ and model limb phase detunings arising as the system adapts (via self-tuning mechanisms) to local surface roughnesses. The whole system operates in the following way. In the absence of a control signal, the limb phases evolve in a random way. Upon the arrival of the signal, it takes the system time Δt to recover (correct) the phase relations according to the motion pattern (Fig. 6b). The parameter h determines how fast the correction is introduced. It should be noted that the remaining blocks of the motion control and coordination system, namely, motion rhythm generator and self-tuning systems, can also be implemented using various dynamical systems. For example, various motion patterns (phase relations for limb motions) can be specified utilizing bistable neurodynamical systems in the form of stable spatial structures of bistable lattices [39].

5. Conclusion

Using the ideas and principles of nonlinear dynamics is, in our view, one of the most important and effective approaches to the study of neuron systems. Dynamic models based on neurophysiological data and concepts open broad possibilities for explaining, predicting, and understanding the dynamic operation mechanisms both of individual neurons and, very importantly, of neuron ensembles and networks of complex architecture. Based on these mechanisms, artificial pattern recognition systems, control systems, new generation computing and information technologies, etc. can be developed. In particular, the principles of neurodynamics seem promising for modeling associative memory processes and spatio–temporal selection, and developing systems for controlling, monitoring, and coordinating motions of autonomous robotic machines.

The following key dynamic mechanisms presented in this talk show the potential of the approach considered.

(1) The study, presented here, of a chain of electrically linked elements (neurons) with nonlinear recovery showed that such a system is capable of producing various spatio–temporal activity structures, including chaotic ones. These structures comprise pulses and excitation fronts, whose instability results in self-maintained oscillations with a certain spatial configuration being established in the system, each element generating a succession of excitation pulses with an element-specific interpulse interval. On the one hand, these structures demonstrate the possibility of oscillations occurring in ensembles whose elements are not self-oscillating (damped oscillations below the excitation threshold). On the other hand, the oscillations performed by the elements of the ensemble turn out to be 'cophased' in a certain way according to a spatio–temporal pattern and in fact form certain information-carrying pulse trains, with information being encoded through variations in the interspike interval.

(2) Based on the self-phase reset effect it is possible to synchronize the oscillations of neuron ensembles. This stimulus-induced synchronization requires no direct contact, or coupling, between the elements, implying that neurons spaced a considerable distance apart can be effectively synchronized by a common pulsed (sensor) stimulus.

(3) Stimuli of various intensities can be used to form cluster structures of spike activity, which are associated, for example, with motor patterns produced by the olive-cerebellar neuron system. Elements of equal oscillation phase

determine the synchronous contraction of various muscular groups of the motor system.

(4) Based on the developed model of an inferior olive neuron, a motion control and coordination system has been proposed for autonomous robotic machines. The basic idea here is to supply the control system with a discrete control block with the function to correct errors arising due to the operation of self-phase reset mechanisms (for motion along a rough surface, for example).

Acknowledgments

The papers underlying in large part this talk were written with coauthors whose valuable contributions are greatly appreciated. This work was supported by a Russian Foundation for Basic Research grant under project No. 06-02-16137.

References

1. Andronov A A, Vitt A A, Khaikin S E *Teoriya Kolebanii* (Theory of Oscillators) (Moscow: Fizmatgiz, 1959) [Translated into English (Oxford: Pergamon Press, 1966)]
2. Andronov A A et al. *Kachestvennaya Teoriya Dinamicheskikh Sistem Vtorogo Poryadka* (Qualitative Theory of Second-Order Dynamic Systems) (Moscow: Nauka, 1966) [Translated into English (New York: J. Wiley, 1973)]
3. Andronov A A et al. *Teoriya Bifurkatsii Dinamicheskikh Sistem na Ploskosti* (Theory of Bifurcations of Dynamic Systems on a Plane) (Moscow: Nauka, 1967) [Translated into English (New York: J. Wiley, 1973)]
4. Andronov A A, in *A.A. Andronov. Sobranie Trudov* (A.A. Andronov. Collected Works) (Ed.-in-Chief M A Leontovich) (Moscow: Izd. AN SSSR, 1956) p. 41
5. Rubin A B *Biofizika* (Biophysics) (Moscow: Knizhnyi Dom Universitet, 1999)
6. Kandel E R, Schwartz J H, Jessell T M (Eds) *Principles of Neural Science* 3rd ed. (New York: Elsevier, 1991)
7. Scott A *Neuroscience: A Mathematical Primer* (Berlin: Springer-Verlag, 2002)
8. Arbib M A *The Metaphorical Brain* (New York: Wiley-Intersci., 1972) [Translated into Russian (Moscow: Editorial URSS, 2004)]
9. Borisyuk G N et al. *Mat. Modelirovanie* **4** (1) 3 (1992)
10. Abarbanel H D I et al. *Usp. Fiz. Nauk* **166** 363 (1996) [*Phys. Usp.* **39** 337 (1996)]
11. Arbib M A, Érdi P, Szentágothai J *Neural Organization: Structure, Function and Dynamics* (Cambridge, Mass.: MIT Press, 1998)
12. Chernavskiĭ D S *Usp. Fiz. Nauk* **170** 157 (2000) [*Phys. Usp.* **43** 151 (2000)]
13. Borisyuk G N et al. *Usp. Fiz. Nauk* **172** 1189 (2002) [*Phys. Usp.* **45** 1073 (2002)]
14. Rabinovich M I et al. *Rev. Mod. Phys.* **78** 1213 (2006)
15. Izhikevich E M *Dynamical Systems in Neuroscience: The Geometry of Excitability and Bursting* (Cambridge, Mass.: MIT Press, 2007)
16. Llinás R, Yarom Y *J. Physiol.* (London) **376** 163 (1986)
17. Elson R C et al. *J. Neurophysiol.* **82** 115 (1999)
18. Golomb D *J. Neurophysiol.* **79** 1 (1998)
19. Leznik E, Makarenko V, Llinás R *J. Nuerosci.* **22** 2804 (2002)
20. Hodgkin A L, Huxley A F *J. Physiol.* (London) **117** 500 (1952)
21. Hindmarsh J L, Rose R M *Proc. R. Soc. London Ser. B* **221** 87 (1984)
22. FitzHugh R *Biophys. J.* **1** 445 (1961)
23. Nagumo J, Arimoto S, Yoshizawa S *Proc. IRE* **50** 2061 (1962)
24. Morris C, Lecar H *Biophys. J.* **35** 193 (1981)
25. Tuckwell H C *Introduction to Theoretical Neurobiology* (Cambridge: Cambridge Univ. Press, 1988)
26. Wilson H R, Cowan J D *Kybernetik* **13** (2) 55 (1973)
27. Ermentrout G B, Kopell N *SIAM J. Math. Anal.* **15** 215 (1984)
28. Kuramoto Y *Chemical Oscillations, Waves, and Turbulence* (Berlin: Springer-Verlag, 1984)
29. Ermentrout G B, Kopell N *SIAM J. Appl. Math.* **46** 233 (1986)
30. Cazelles B, Courbage M, Rabinovich M *Europhys. Lett.* **56** 504 (2001)
31. Rulkov N F *Phys. Rev. E* **65** 041922 (2002)
32. Nekorkin V I, Vdovin L V *Izv. Vyssh. Uchebn. Zaved. Prikl. Nelin. Dinamika* **15** (5) 36 (2007)
33. Courbage M, Nekorkin V I, Vdovin L V *Chaos* **17** 043109 (2007)
34. Rubin J, Bose A *Network* **15** (2) 133 (2004)
35. Kazantsev V B et al. *Phys. Rev. E* **68** 017201 (2003)
36. Kazantsev V B, Nekorkin V I, in *Nelineinye Volny 2002* (Nonlinear Waves 2002) (Exec. Eds A V Gaponov-Grekhov, V I Nekorkin) (N. Novgorod: IPF RAN, 2003) p. 9
37. Kazantsev V B *Phys. Rev. E* **64** 056210 (2001)
38. Nekorkin V I et al. *Mat. Modelirovanie* **17** (6) 75 (2005)
39. Nekorkin V I, Velarde M G *Synergetic Phenomena in Active Lattices* (Berlin: Springer-Verlag, 2002)
40. Nekorkin V I, Shchapin D S, Dmitrichev A S *Izv. Vyssh. Uchebn. Zaved. Prikl. Nelin. Dinamika* **15** (1) 3 (2007)
41. Nekorkin V I et al. *Physica D* (submitted)
42. Henze D A, Buzsáki G *Int. Congress Ser.* **1250** 161 (2003)
43. Welsh J P et al. *Nature* **374** 453 (1995)
44. Leznik E, Makarenko V, Llinás R *J. Nuerosci.* **22** 2804 (2002)
45. Kazantsev V B et al. *Proc. Natl. Acad. Sci. USA* **101** 18183 (2004)
46. Kazantsev V B et al. *Proc. Natl. Acad. Sci. USA* **100** 13064 (2003)
47. Kazantsev V B, Nekorkin V I, in *Nelineinye Volny 2004* (Nonlinear Waves 2004) (Exec. Eds A V Gaponov-Grekhov, V I Nekorkin) (N. Novgorod: IPF RAN, 2005) p. 345
48. Llinás R R *I of the Vortex: From Neurons to Self* (Cambridge, Mass.: MIT Press, 2001)
49. Kazantsev V B, Nekorkin V I *Izv. Vyssh. Uchebn. Zaved. Prikl. Nelin. Dinamika* **9** (1) 38 (2001)

PACS numbers: **05.45.–a**, **87.10.+e**, 87.19.La
DOI: 10.1070/PU2008v051n03ABEH006494
DOI: 10.3367/UFNr.0178.200803h.0323

Modeling nonlinear oscillatory systems and diagnostics of coupling between them using chaotic time series analysis: applications in neurophysiology

B P Bezruchko, V I Ponomarenko,
M D Prokhorov, D A Smirnov, P A Tass

1. Introduction

Using time series of experimental observables to identify and estimate interaction parameters between sources of complex (chaotic) oscillations [1–3] is a task of relevance to many disciplines, from physics and biology to geophysics, medicine, and engineering. A vibration analysis of machine elements can identify the source of the vibrations [4], whereas identifying interactions between various brain regions based on multichannel electroencephalogram analysis benefits epilepsy patients by locating the sites of pathological activity [5]. Particular attention in this area is paid to irregular signals because it is a long-recognized fact that the chaotic behavior of nonlinear systems is typical [3, 6, 7].

Reflecting the diversity of possible situations and the factors of noise and nonstationarity, a wide variety of approaches to identifying and assessing the 'intensity' of a coupling have been developed using mathematical statistics and spectral analysis [1], information theory [8, 9], and nonlinear dynamics [5, 10–12]. Among the most widely-used of these are the calculation of cross-correlation functions and of coherence functions [1], event sequence analysis with time series [13], the estimation of nearest neighbor distribution in the space of states [5], and the determination of characteristics of 'information transfer' between signals [8]. Whereas the techniques listed above process a signal